Study on Mechanism of Segmental Lining-Bolt Combined Support for Deep-Buried Tunnel

Ming-yang Ren · Qiang-yong Zhang · Zhen-jie Zhang · Long-yun Zhang · Qiang Gao

Abstract Segmental lining-bolt combined support is extensively applied in mechanized shield tunneling for deep tunnel. In order to reveal the mechanism of segmental lining-bolt combined support, a true three-dimensional geo-mechanical model test and numerical simulation study are conducted on the background of Xianglushan Tunnel in the Yunnan Water Diversion Project. The research results show that: (1) the mechanism of segmental lining-bolt combined support includes two aspects: "load bearing effect" and "protection and reinforcement effect". The segmental lining is a kind of rigid support and mainly plays a load-bearing role. The bolt reinforces and protects the surrounding rock, whose load-bearing effect is not obvious; (2) the fault has a distinct influence on the bearing capacity of the surrounding rock. The loads taken by the surrounding rock and the support is significantly different under different geological conditions; (3) the plastic zone causes the surrounding rock stress to move to deep rock mass, which induces the formation of pressure arch. The larger the size of plastic zone is, the larger the range of pressure arch formed in deep rock mass is, and the farther the distance from pressure arch to tunnel wall is. The plastic zone is the necessary condition for the formation of pressure arch. The research results can provide the basis for the establishment of construction scheme and the optimization of support design for large buried tunnel under complex geological conditions.

1 Introduction

With the development of underground engineering technology, more and more deep-buried, extra-long and long-span tunnels increased considerably. Under the influence of high ground stress, high external water pressure, high ground temperature and excavation disturbance, the physical and mechanical properties of deep rock mass are obviously different from those of shallow rock mass, which often leads to support problems in deep tunnel (He et al. 2009; Xie 2017). It is difficult to maintain the stability of surrounding rock by the single support. So it is usually necessary to adopt a variety of different types of support structures to cooperate, that is, combined support technology.

As a common combined support technology, lining-bolt combined support has been widely used in engineering fields such as transportation, energy, mining and hydropower (Cao 2014; Gao et al. 2007; Holmgren and Ansell 2006; Huang et al. 2011; Wang

M. Ren (✉) · Q. Zhang · Z. Zhang · L. Zhang · Q. Gao
Geotechnical and Structural Engineering Research Center,
Shandong University, Jinan 250061, Shandong, China
e-mail: 865812512@qq.com

et al. 2014; Yang 2015). However, due to the complexity and uncertainty of geotechnical engineering problems, the study on the mechanism of lining-bolt combined support is far behind the engineering practice. The design of support structure is still based on the empirical design method. Funatsu et al. (2008) adopted the discrete element method to study the support effect of lining-bolt combined support on surrounding rock in shallow buried sand tunnel, and revealed the formation mechanism of pressure arch in loosely fractured surrounding rock. Oliveir and Diederichs (2017) analyzed the failure mode of fractured sandstone tunnel by field test, and studied the support mechanism of shotcrete lining and bolt by numerical method. A composite supporting ring model (Sun and Zhang 2016) including three parts: bolt reinforcement ring, primary lining ring and second lining ring is established, and the support mechanism of each supporting ring is studied by theoretical analysis method. Cheng (2014) points out that the bonding effect and deepening effect of shotcrete lining-bolt combined support can improve the mechanical parameters of surrounding rock and enhance the self-bearing capacity of surrounding rock by performing the geo-mechanical model test on Huangdao Groundwater Sealing Rock Reservoir. Sun et al. (2004) finds that shotcrete lining-bolt combined support can improve the strength of surrounding rock and help surrounding rock form pressure arch to stimulate the self-bearing capacity of surrounding rock. According to the characteristics of bolt-shotcrete lining-steel frame combined support, the mechanical model (Wen et al. 2015) of composite arch with system bolt as supporting outer arch, shotcrete lining and steel frame as supporting inner arch is established, and the interaction mechanism and load-bearing relationship of two-layer arch are studied. Hu et al. (2018) proposes a support technique of segmental lining combined with compressible ceramsite layer and bolt for shield tunnel in layered rock mass, and studies the mechanism of segmental lining and bolt by model test. However, the current research results on the mechanism of lining-bolt combined support are mostly focused on the primary lining (shotcrete)—bolt combined support in shallow tunnel. There are few studies on the mechanism of segmental lining-bolt combined support in large buried tunnel under complex geological conditions. Moreover, the previous study on segmental lining usually ignores surrounding rock. The oversimplified structural mechanics method is often adopted to study the mechanical response of segmental lining (Arnau and Molins 2011; Barzegar et al. 2015; El Naggar et al. 2008; Lee and Ge 2001; Molins and Arnau 2011), or more accurate segment contact models (Salemi et al. 2015) are proposed to modify the calculation method of segmental lining structure response.

In this paper, a true three-dimensional geo-mechanical model test on the segmental lining-bolt combined support for the deep diversion tunnel through a weak fault is carried out, which is based on the background of Xianglushan tunnel in Yunnan Water Diversion Project, China. The stress and deformation of surrounding rock and segmental lining, the distribution law of the bolt axial force, the rock-bolt interface stress are analyzed. Combined with numerical simulation, and the model test results are verified and complemented. In general, research results can provide the basis for the establishment of construction scheme and the optimization of support structure design in large buried tunnel under complex geological conditions.

2 Project Overview

Yunnan Water Diversion Project is located in the southeast of the Qinghai-Tibet Plateau, with a total length of 663.23 km, which is a regional long-distance water diversion project. Xianglushan Tunnel is located at the first section of main drainage line of Yunnan water diversion project. It crosses the watershed between Jinsha River and Lancang River. The lithology and geological conditions are very complicated. Folds and faults are developed along the tunnel. The stability of surrounding rock is poor. The Xianglushan Tunnel, with a total length of 63.426 km, originates from Shigu and ends in Songgui. The ground elevation along the tunnel is generally 2400–3400 m, and the maximum buried depth is 1412 m. Many regions have high to extremely high stress background. It is a dominant engineering of the whole Yunnan Water Diversion Project.

In this paper, typical deep buried region (DL37 + 845–DL37 + 915) in Xianglushan Tunnel is selected. The average depth of the tunnel is about 1000 m, whose section is circular, and the diameter of the tunnel is 10 m. The region contains an inclined

weak fault about 15 m wide with dip angle 65°. The direction of the tunnel is approximately orthogonal to the weak fault. The surrounding rock in the fault is mainly silty mudstone, and the uniaxial compressive strength is less than 20 MPa, which belongs to typical soft rock. The front and back sides of the fault are limestone, and belong to Class III surrounding rocks with relatively complete rock mass structure. The uniaxial compressive strength is about 70 MPa, and it belongs to hard rock. The selected region contains not only typical soft rock and hard rock, but also the intersection of soft rock and hard rock, whose geological conditions are very complicated.

3 Similarity Principle and Development of Model Test Materials

3.1 Similarity Principle

The similarity principle (Zhang et al. 2008) of geo-mechanical model test means that the important physical phenomena in the model should be similar to the prototype. For instance, the model material, shape and load are required to follow certain conditions.

According to the equilibrium equation, the geometric equation, the constitutive equation, the stress and the displacement boundary condition, the following similar relationship of the geo-mechanical model test can be derived.

(1) Stress similarity ratio C_σ, unit weight similarity ratio C_γ and geometric similarity ratio C_L should satisfy the relationship

$$C_\sigma = C_\gamma C_L \qquad (1)$$

(2) Displacement similarity ratio C_δ, geometric similarity ratio C_L and strain similarity ratio C_ε should satisfy the relationship

$$C_\delta = C_L C_\varepsilon \qquad (2)$$

(3) Stress similarity ratio C_σ, elastic modulus C_E and strain similarity ratio C_ε should satisfy the relationship

$$C_\sigma = C_E C_\varepsilon \qquad (3)$$

(4) The geo-mechanical model test also requires that the similar ratio of all dimensionless physical quantities (such as strain, internal friction angle, Poisson's ratio, etc.) is equal to 1. The similar ratio of the same dimension physical quantity is equal, i.e.

$$C_\varepsilon = C_\phi = C_\upsilon \qquad (4)$$

$$C_\sigma = C_E = C_c \qquad (5)$$

According to the size of the model test device (0.7 m × 0.7 m × 0.7 m), the geometric similarity ratio of the model test is determined to be CL = 100 in order to reduce the influence of the model boundary. So the actual simulation range is 70 m × 70 m × 70 m. The prototype dimensions and model dimensions of surrounding rock and support structure are respectively shown in Fig. 1a, b.

3.2 The Development of Model Test Materials

The similar material (Zhang et al. 2018) for surrounding rock is a kind of composite material containing iron ore powder, barite powder, quartz sand and rosin alcohol solution according to the corresponding proportion. It has the advantages of stable performance, simple manufacturing process and non-toxic and harmless. In this study, the unit weight similarity ratio is 1, so the stress similarity ratio is 100 according to the geometric similarity ratio 100. Through a large number of similar material mechanical tests, and the physical and mechanical parameters of model material and prototype surrounding rock are shown in Table 1, and the determined proportion of components of model similar materials is shown in Table 2.

The similar material of lining is made of gypsum powder by changing the proportion of water. Lining is often considered as elastic material in design, so the modulus of elasticity, uniaxial compressive strength and uniaxial tensile strength are selected as the main mechanical index for the adjustment. After a large amount of proportioning tests, the weight ratio of water to gypsum powder that basically meets the requirements of lining material is 1:1.6.

According to the previous study (Li et al. 2011), the model bolt is selected according to the principle of stiffness similarity. In this test, ABS (Acrylonitrile Butadiene Styrene plastic) material is used to simulate the bolt, which has the characteristics of high strength, good toughness and easy processing and forming.
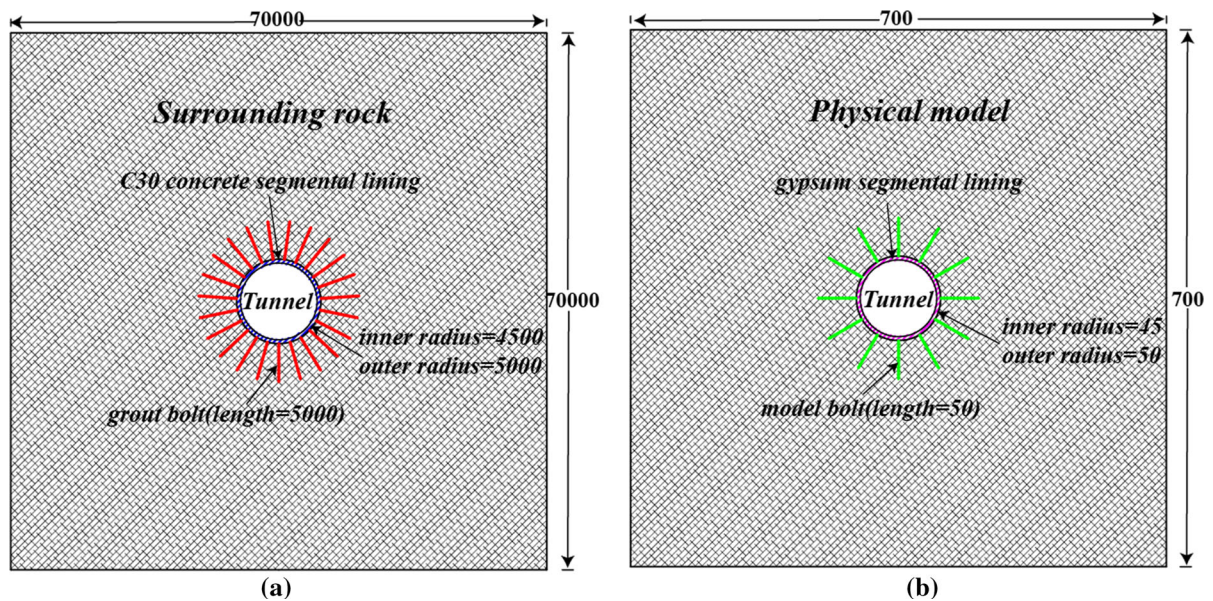
Fig. 1 Prototype dimensions and model dimensions of surrounding rock and support (unit: mm). **a** Prototype dimensions; **b** Model dimensions

Table 1 Physical and mechanical parameters of surrounding rock

	Lithology	Density (kg/m³)	Modulus of deformation (MPa)	UCS (MPa)	UTS (MPa)	Cohesion (MPa)	Friction angle (°)	Poisson's ratio
Prototype	Limestone	2650	25.3e3	64.8	4.5	11.4	54.5	0.28
	Silty mudstone	2550	6.8e3	16.3	1.3	4	33	0.3
Model	Limestone	2620–2680	228.6–285.2	0.61–0.69	0.042–0.047	0.11–0.16	51.8–55.4	0.26–0.28
	Silty mudstone	2480–2560	53.4–69.3	0.15–0.21	0.011–0.018	0.031–0.044	33–39	0.27–0.30

Table 2 Proportioning schemes of similar materials for surrounding rock

Category	Material proportion[a] I:B:S	Concentration of alcohol rosin solution (%)	Cementation agent[b] percentage of aggregate[c] weight (%)
Similar material of limestone	1:0.5:0.5	8	5.5
Similar material of silty mudstone	1:0.67:0.55	2.5	5.5

[a]I represents iron ore powder, B represents barite powder, S represents quartz sand. All quantities are measured in weight units

[b]Cementation agent is the solution of rosin dissolved in alcohol

[c]Aggregate contains iron ore powder, barite powder and quartz sand

Because of the compactness of the prototype bolt arrangement (longitudinal spacing 1.25 m) and the small diameter (28 mm), the spacing and diameter of the bolt can't be scaled strictly according to the geometric similarity ratio except the length of the bolt.

Therefore, the bolts on each section in physical model are equivalent to the bolts within 5 m in the longitudinal direction for the practical engineering. According to the system bolt layout of the prototype and model in Fig. 1a, b, one model bolt is approximately

equivalent to ten prototype bolts in the model test. According to Eq. (6), the stiffness similarity ratio of bolt is 1e4. When the length of model bolt is 50 mm, the diameter of the model bolt can be determined to about 3 mm.

$$C_K = \frac{(EA/L)_P}{(ea/l)_m} = \frac{E_p}{e_m} \frac{A_p}{a_m} \frac{l_m}{L_p} = \frac{C_E C_L^2}{C_L} = C_E C_L = 1e4$$

(6)

The similar material of grout is simulated by the mixture of gypsum powder, quartz sand and water. The grout material in the field is M30 cement mortar. In this test, the uniaxial compressive strength, tensile strength and modulus of elasticity are selected as the main mechanical index for the proportion adjustment. Through an amount of proportioning tests, the weight ratio of gypsum powder, quartz sand and water which basically meet the requirements of grout is 1:0.8:1.4.

4 Geo-Mechanical Model Test

4.1 Model Test Scheme Design

In order to study the mechanism of segmental lining-bolt combined support under complex geological conditions, two geo-mechanical model test schemes are designed in Table 3.

4.2 Model Test Device

The model test device is shown in Fig. 2. Its external dimension is 2.0 m × 1.75 m × 1.75 m, and its internal dimension is 0.7 m × 0.7 m × 0.7 m. It is mainly composed of three parts: reaction platform system, intelligent hydraulic loading system and automatic test data acquisition system. The reaction platform system consists of a modular combined reaction device, loading plate, guide frame, etc. The intelligent hydraulic loading system can monitor the output pressure value of each hydraulic cylinder through the real-time recording software and adjust the output pressure of the multi-way hydraulic station. Therefore, the true three-dimensional ground stress state for the deep tunnel is accurately simulated. The model test data automatic acquisition system is mainly composed of multi-point displacement data automatic acquisition system, strain data automatic acquisition system and stress data automatic acquisition system, which is used to automatically collect the displacement, stress and strain during the model test.

4.3 Physical Model Building

The whole physical model is built by statically compacting materials layer by layer. The basic process includes: (1) Install fault making device; (2) Compound the model materials in front of the fault, behind the fault and in the fault; (3) Lay the model material evenly and compact them preliminarily; (4) Remove the fault making device and compress the similar material further; (5) Air drying and maintenance; (6) Repeat the above operations (1)–(5) until the model building is completed.

The general procedures of making fault are shown in Fig. 3. Firstly, the fault clapboard is placed to the corresponding location and fixed on the guide frame with the fixing plate. Then, the model materials are poured to the corresponding part. After preliminary compaction, remove the fault making device and compress the similar material further. Finally, air dryer is used for maintenance.

By the above process, the physical model satisfying test scheme 1 can be produced. However, due to the limitation of the true three-dimensional geo-mechanical model test device, the size of the model tunnel and the bolt installing technology, the method of pre-embedded bolt is adopted for test scheme 2.

The lining segment is prefabricated by the segmental lining mould (Fig. 4a). The method of

Table 3 Model test schemes

Test scheme	Test type	Test purpose
Scheme 1	Excavation + segmental lining	Study mechanism of segment lining support
Scheme 2	Excavation + segmental lining + bolt	Study mechanism of segment lining-bolt combined support

Fig. 2 Geo-mechanical model test device

prefabricating lining segment is: After mixing the special gypsum powder and water evenly, inject the mixed gypsum solution into the segment mould. In order to make gypsum solution compact, the mold should be placed on the vibrating table. Then take it to the ventilation. Finally dismantle the mold and take the lining segment. The prefabricated lining segments are shown in Fig. 4b.

4.4 Layout of Measuring Points and Installation of Test Elements

In order to capture the stress and deformation of surrounding rock and support structure, four typical monitoring sections are selected with multi-point displacement meter, micro-pressure cell and miniature strain brick, which are shown in Fig. 5. The monitoring section 1 is located in hard rock above the fault, the monitoring section 2 is located in the intersection of soft rock and hard rock, the monitoring section 3 is located in soft rock, and the monitoring section 4 is located in hard rock below the fault. Each main monitoring section consists of two sub-monitoring sections: the deformation monitoring section (the blue line in Fig. 5) and the stress monitoring section (the green line in Fig. 5). Because the axis of the tunnel is orthogonal to the fault, according to the symmetry,

there are five survey lines laid out in the upper half of each monitoring section. Each surveying line is arranged with four measuring points. The distances of the four measuring points from the tunnel wall are 5, 30, 100 and 200 mm, respectively. The detailed arrangement is shown in Fig. 6.

In order to monitor the contact pressure between the surrounding rock and the segmental lining and the interface stress on the bolt surface and grout surface, the measuring points layout of the segmental lining and bolt for the above four monitoring sections is shown in Fig. 7.

4.5 Model Excavation and Segmental Lining Support Scheme

In order to simulate the whole process of tunnel construction in actual rock mass realistically, the model test construction includes three stages.

(1) Preloading stage. According to Eq. (7), the ground stress in prototype and model can be calculated. Then, the physical model is loaded gradually by the numerical control hydraulic loading system. Preloading stage is to create a true three-dimensional initial stress field in the physical model.
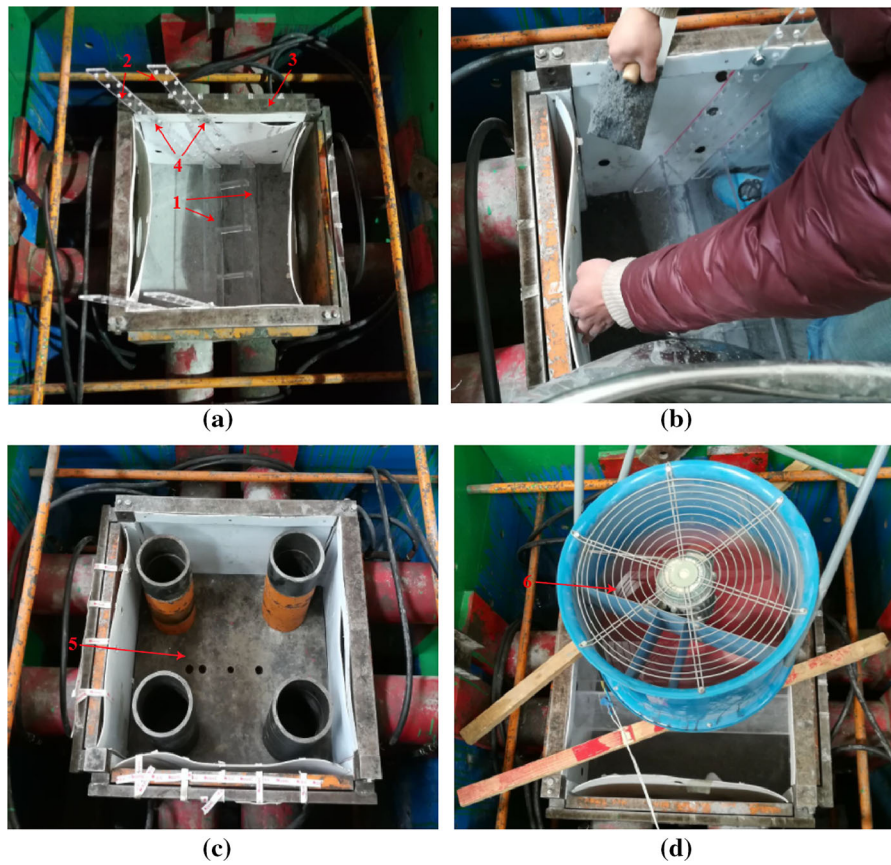
Fig. 3 The general procedures of making fault. **a** Fault making device; **b** Pouring the model material; **c** Compacting the model material; **d** maintaining the model. 1-fault clapboard; 2-fixing plate; 3-guide frame; 4-fixing bolt; 5-compaction plate; 6-air dryer

Fig. 4 Prefabrication of segmental lining. **a** Segmental lining mould; **b** Prefabricated lining segment

$$\begin{cases} \sigma_H = 1.4 \cdot \gamma H, \sigma_h = 1.02 \cdot \gamma H & H \leq 400\,\text{m} \\ \sigma_H = 1.2 \cdot \gamma H, \sigma_h = 0.74 \cdot \gamma H & H > 400\,\text{m} \\ \sigma_v = \gamma H \end{cases} \quad (7)$$

where σ_H is the maximum horizontal stress, σ_h is the minimum horizontal stress, σ_v is the vertical stress, which equals to the self-weight stress of rock mass γ is the unit weight of rock (0.0265MP/m), H is the depth

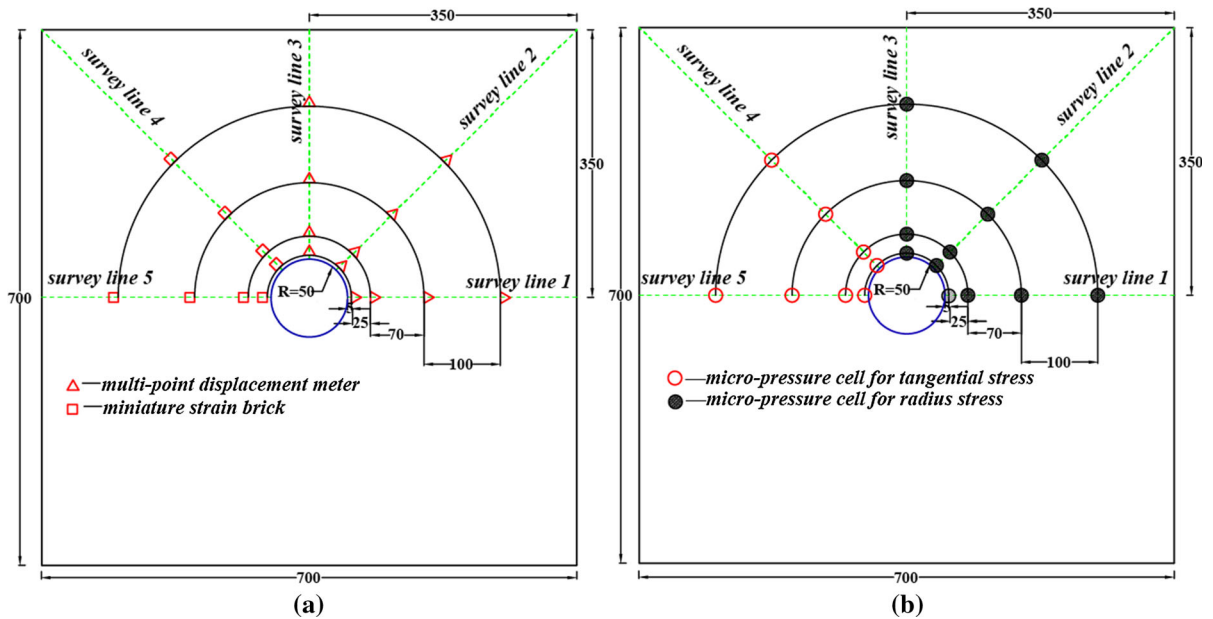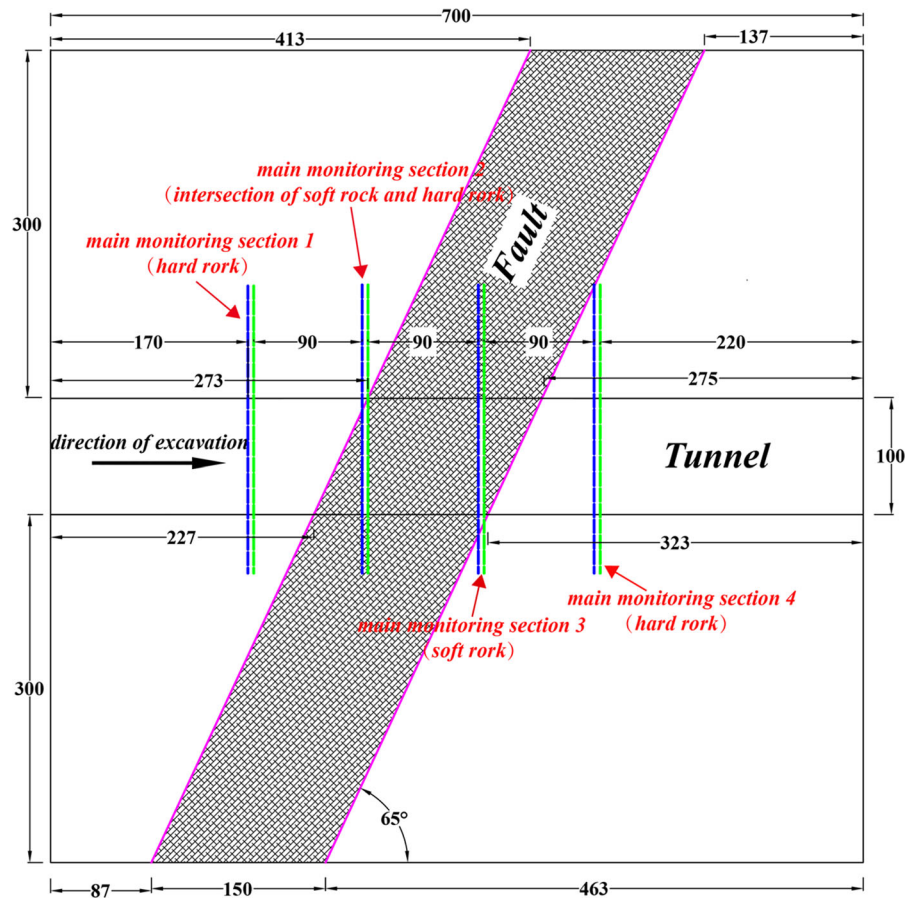**Fig. 5** Layout of monitoring sections in the surrounding rock (unit: mm)

Fig. 6 Layout of measuring points (unit: mm). **a** Deformation measuring points; **b** Stress measuring points
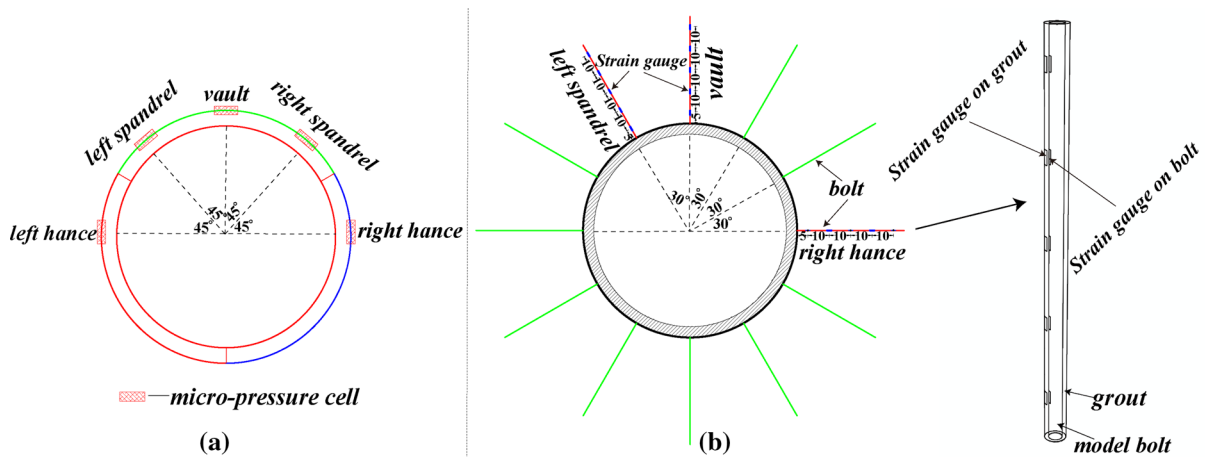
Fig. 7 Layout of measuring points on the segmental lining and bolt (unit: mm). **a** Measuring points on the segmental lining; **b** Measuring points on the bolt

(unit: m). The minimum horizontal stress is parallel to the tunnel axial and the maximum horizontal principal stress is perpendicular to the tunnel axial.

(2)   Excavation stage. The excavation and support of tunnel are carried out according to the actual construction. After preloading stage, excavate and trim the model tunnel with the excavation tool. The first excavation length is 80 mm.

(3)   Segmental lining installation stage. The segmental lining installation is carried out by the method of "piecewise installation, piecewise splicing". Firstly, use the segment installation tool to place the segment on the bottom left side of the excavated tunnel, and then take out the segment installation tool after the surrounding rock and the segment are bonded stably. In accordance with the above method, the bottom right segment is placed successively, and the top segment is finally installed. In order to integrate the segment with the neighboring segments, thin quick-drying structural adhesive should be applied to longitudinal joint and hoop joint between adjacent segments. The width of the lining segment is 50 mm, so the length of each segmental lining installation is 50 mm.

After completing the first excavation and support, the second construction step begins. The construction footage is 50 mm, that is, 50 mm for each excavation, and 50 mm for subsequent support. The excavation and support are repeated continuously, thus realizing the progressive advancement of tunnel excavation and support.

4.6 Model Test Results

The displacement and stress obtained from model test have been transformed into prototype displacement and stress according to similarity principle. Because the distributions of surrounding rock stress and displacement for four monitoring sections are similar, the results are analyzed by taking typical monitoring section 1(hard rock) and monitoring section 3(soft rock) as examples.

4.6.1 Displacement Field of Surrounding Rock

The surrounding rock radial displacement curves with the distance from the tunnel wall are shown in Fig. 8, from which, it can be seen that:

(1)   After excavation, the surrounding rock around the tunnel shrinks into the tunnel. The closer the distance from surrounding rock to the tunnel wall is, the larger the radial displacement of the surrounding rock is. The displacement of the surrounding rock within the range of 1.0D (D is the tunnel diameter) is significantly affected by excavation.

(2)   The distribution law of radial displacement for the two test schemes is basically the same. Compared with test scheme 1, the deformation of surrounding rock around the tunnel is reduced
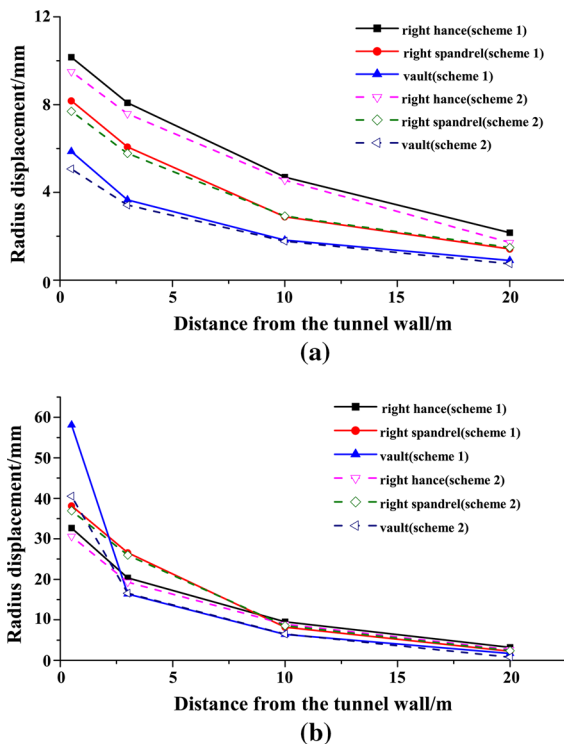
Fig. 8 Radial displacement curves with the distance from the tunnel wall. **a** Monitoring section 1; **b** Monitoring section 3

when the segmental lining-bolt combined support is adopted in test scheme 2. The deformation of surrounding rock in hard rock (monitoring section 1) decreases by about 11%, and that of soft rock (monitoring section 3) decreases by about 11%. Moreover, the displacement of the surrounding rock at the vault decreases the most, the average is about 28%, and the displacement of the surrounding rock at the hance decreases the least, the average is about 5%.

(3) For test scheme 1, along the radial direction of the tunnel, the displacement curves of surrounding rock near the tunnel change steeply, especially the surrounding rock at the vault in soft rock. However, for test scheme 2, the displacement curves of surrounding rock around the tunnel are gentler. Moreover, the displacement of surrounding rock decreases greatly within the range of bolt reinforcement, and the displacement of surrounding rock beyond the range of bolt reinforcement is basically the same for the two schemes. The reason is that the bolt

improves the mechanical properties of the surrounding rock within the reinforcement range, and the integrity of the surrounding rock is significantly enhanced when the segmental lining-bolt combined support is adopted.

4.6.2 Stress Field of Surrounding Rock

Figure 9 shows the radial stress curves and tangential stress curves of surrounding rock with the distance from the tunnel wall. Table 4 shows the stress release rate of surrounding rock at the excavation time and the lining support time. The stress release rate of surrounding rock refers to the percentage of the radial stress release value of surrounding rock and its original stress at the excavation time or lining support time for the corresponding monitoring section. The radial stress release value of surrounding rock is the original radial stress minus the current radial stress.

From Fig. 9 and Table 4, it can be seen that

(1) The stress variation trend of surrounding rock around the tunnel is basically the same for two test schemes after the completion of tunnel construction. Radial stress of surrounding rock around the tunnel is released, and the closer the distance from surrounding rock to the tunnel wall is, the smaller radial stress of surrounding rock is. The tangential stress concentration occurs in hard rock (monitoring section 1), and the closer the distance from surrounding rock to the tunnel wall is, the larger the tangential stress of surrounding rock is. With the distance from the tunnel wall increasing, the tangential stress gradually reduces to the original stress. Because the monitoring section 3 is located in soft rock, the rock mass strength is low, and the surrounding rock near the tunnel is in the post-peak softening stage after excavation. So the tangential stress of surrounding rock increases first and then decreases with the distance from the tunnel wall, and the stress of surrounding rock moves to the deep rock mass to form a certain range of pressure arch. Overall, the stress of surrounding rock is significantly affected by excavation disturbance within the range of 1.0D (D is the tunnel diameter), which is consistent with the result of displacement field.
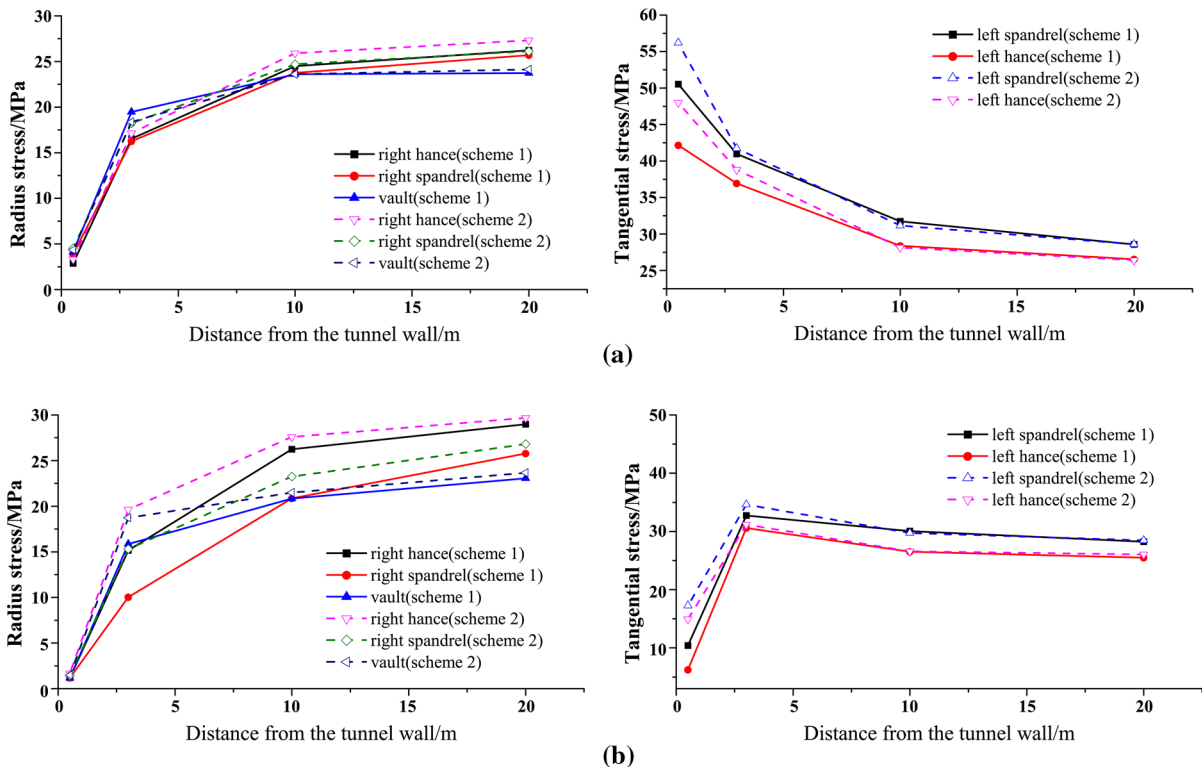
Fig. 9 Stress curves with the distance from the tunnel wall. **a** Monitoring section 1; **b** Monitoring section 3

Table 4 Radial stress release rate of surrounding rock on monitoring sections at excavation time and lining time

Monitoring section	Location of monitoring section	Location on the tunnel	Excavation time		Lining time	
			Scheme 1 (%)	Scheme 2 (%)	Scheme 1 (%)	Scheme 2 (%)
1	Hard rock	Right hance	30	23	81	72
		Right spandrel	28	28	79	79
		Vault	29	11	86	64
2	Soft rock	Right hance	72	66	97	94
		Right spandrel	78	62	97	92
		Vault	77	72	96	95

(2) The radial stress release rates of the surrounding rock at the excavation time and lining support time under different geological conditions are obviously different. For test scheme 1, the radial stress release rate of surrounding rock in soft rock is larger at excavation time and support time, which is about 76% and 97% respectively, while that of the surrounding rock in hard rock is smaller, which is about 29% and 82% respectively.

(3) Compared with test scheme 1, both the radial stress and tangential stress of surrounding rock under different geological conditions increase when the method of segmental lining-bolt combined support is adopted in test scheme 2. However, the radial stress release rate of surrounding rock decreases regardless of excavation time or lining support time compared with scheme 1. The average stress release rate of surrounding rock in hard rock at excavation

time and lining support time is reduced by about 8% and 10%, respectively. The average stress release rate of surrounding rock in soft rock is reduced by 9% and 3%, respectively. It can be seen that the bolt can significantly enhance the mechanical properties and bearing capacity of surrounding rock and improve the stability of surrounding rock.

4.6.3 Contact Pressure Between Surrounding Rock and Segmental Lining

Distribution curves of contact pressure between surrounding rock and segmental lining after tunnel construction for two test schemes are shown in Fig. 10. From Fig. 10, it can be seen that

(1) After the tunnel construction, the contact pressure of each location around the tunnel under different geological conditions is different. The maximum contact pressure does not exceed 1 MPa. In general, the contact pressure at the vault and the spandrel is larger than that of the hance. The maximum contact pressure between the surrounding rock and segmental lining in hard rock is located at the spandrel, and the maximum contact pressure in soft rock is located at the vault.

(2) Compared with the test scheme 1, the contact pressure around the tunnel is more uniform, and the contact pressure around the tunnel under different geological conditions is reduced for test scheme 2. On the whole, the integrity of the surrounding rock is also greatly enhanced after bolt reinforcement.

4.6.4 Bolt axial Force and Interface Stress

Transform the strain monitored in test scheme 2 into the bolt axial force, and the distribution curve of the bolt axial force is shown in Fig. 11. The interfaces include the bolt-grout interface and the grout-surrounding rock interface, which are simply referred to as the bolt surface and the grout surface for convenience of description. The interface shear stress on the bolt surface can be solved according to the following Eq. (8).
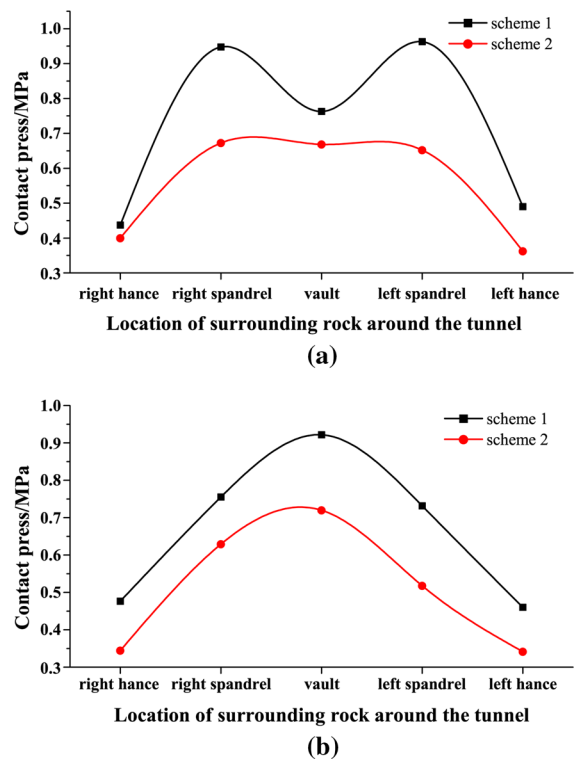

Fig. 10 Distribution curves of contact pressure between surrounding rock and segmental lining. **a** Monitoring section 1; **b** Monitoring section 3

$$\tau_i = \frac{N_i - N_{i+1}}{\pi \phi \Delta l_i} \qquad (8)$$

where N_i and N_{i+1} are bolt axial forces at two adjacent strain gauges, ϕ is the bolt diameter, Δl_i is the distance of two adjacent strain gauges. For the solution of the interface shear stress on grout surface, refer to the previous research (Zhang and Yin 2009), the grout and bolt is considered as a composite rod. Calculate the axial force of the composite rod firstly, and then calculate the interface shear stress of the grout surface according to the Eq. (8). The obtained interface shear stress distribution curves on the bolt surface and the grout surface are shown in Fig. 12, in which the blue dotted line represents the interface shear stress on the bolt surface and the red solid line represents the interface shear stress on the grout surface.

From Figs. 11 and 12, it can be seen that

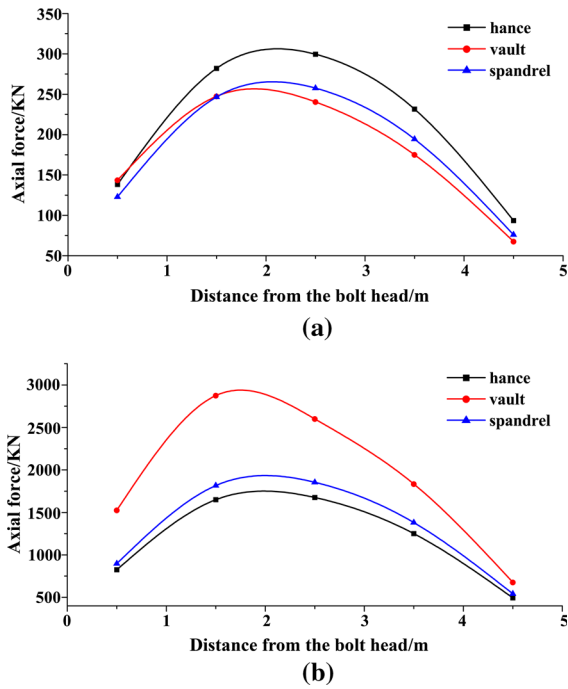(1) The axial force of all bolts around the tunnel under different geological conditions is tensile,

Fig. 11 Distribution curves of the bolt axial force. **a** Monitoring section 1; **b** Monitoring section 3

Fig. 12 Interface shear stress distribution curves of the bolt surface and the grout surface. **a** Monitoring section 1; **b** Monitoring section 3

and it is distributed in the form of "small at both ends of bolt, large in the middle of bolt". That is, the axial force increases sharply at first, and then decreases sharply after the peak value along the bolt. However, the distribution of interface shear stress on the bolt surface and grout surface is just the opposite, which is in the form of "large at both ends of bolt, small in the middle of bolt". The interface shear stress distribution curves from bolt head to bolt tail vary from negative to positive, and the inflection point of the curve is located at the zero point of interface stress, i.e. the neutral point position.

(2) Two types of interface shear stresses are distributed on both sides of the neutral point. One is the drawing shear stress caused by the shrinkage of the surrounding rock to the tunnel, located on the side close to the tunnel. The other is the bonding shear stress on the interface in the deep part of the surrounding rock, which is caused by the drawing shear stress. The resultant forces of the two types of interface shear stresses are equal in magnitude but opposite in direction. The drawing shear stress acts to restrain the deformation of the surrounding rock, and the
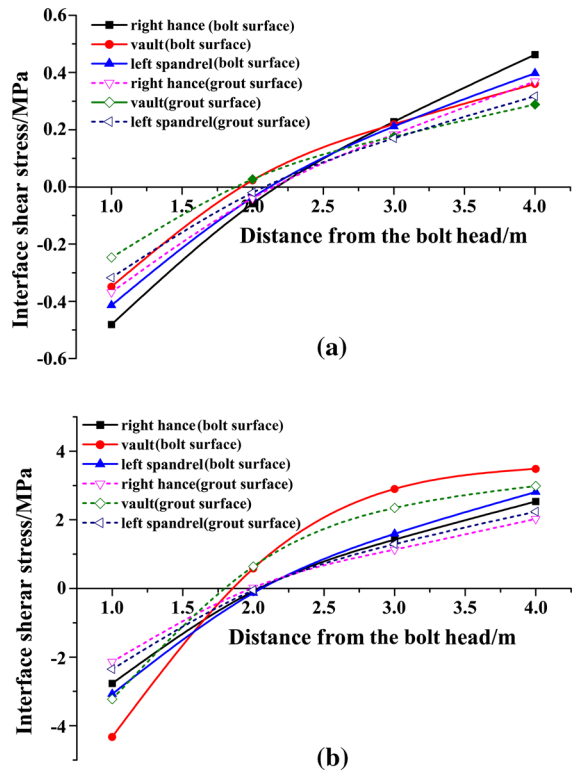
bonding shear stress connects the shallow rock mass and the deep rock mass in series to form a unity and transfers the stress to the deep rock mass.

(3) When the surrounding rock shrinks into the tunnel, the stress transfers from the surrounding rock to the grout first, and then the stress transfers from the grout to the bolt. The bolt axial force is caused by the interface shear stress between the grout and the bolt, and the interface shear stress between the grout and the bolt is caused by the interface shear stress between the surrounding rock and the grout. Therefore, the distribution and magnitude of the bolt axial force are related to the distribution and magnitude of the two types of interface shear stresses. In hard rock, the bolt axial force and interface shear stress around the tunnel are basically the same and small. However, the axial force and interface shear stress of the bolts are all relatively large in soft rock. The axial force

and interface shear stress of the bolt at the vault are the largest. Combined with the law of the displacement field and stress field of the surrounding rock, it can be seen that the surrounding rock in soft rock is in the plastic state after excavation, and the excessive plastic deformation significantly increases the axial force and interface shear stress of the bolts around the tunnel.

5 Numerical Simulation

Although the stress and deformation of surrounding rock and support for large buried tunnel under complex geological conditions are analyzed through model tests, the results obtained are only based on a limited number of monitoring points. It is difficult to fully understand the information on the surrounding rock excavation disturbance zone, the deformation and stress of surrounding rock and support. Therefore, in order to deeply study the mechanism of segmental lining-bolt combined support for deep tunnel under complex geological conditions, the numerical simulation of model test construction process is carried out by the finite difference procedure. The calculated results and test results are comparatively analyzed, with a view to verifying each other and discovering some general laws.

5.1 Numerical Model and Calculation Parameters

The size of the numerical model is consistent with the extent of the physical model. The direction of the tunnel axis is the Y-axis direction, the horizontal direction perpendicular to the tunnel axis is the X-axis direction, and the vertical direction is the Z-axis direction. The three-dimensional numerical model established is shown in Fig. 13. The location and occurrence of the fault are the same as that in the test. The whole model contains 92,532 hexahedral elements and 97,241 nodes. Normal displacement constrained boundary conditions are applied to the four sides and the bottom of the model, and normal stress is applied to the top surface to simulate the self-weight of overlying rock mass. The stress field of the model is calculated according to Eq. (7) and initialized according to the stress similarity ratio.
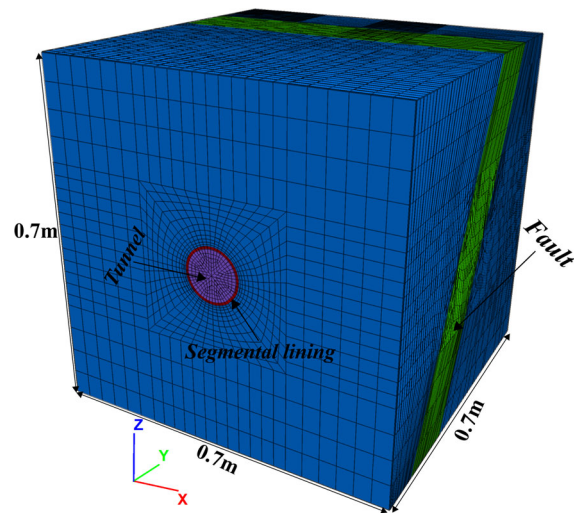

Fig. 13 Three-dimensional numerical model

The surrounding rock and segmental lining are simulated by solid elements. The strain softening model based on Mohr–Coulomb yield criterion is adopted for the surrounding rock, and linear elastic model is adopted for the segmental lining. The interface between surrounding rock and segmental lining is simulated by interface element, and the bolt is simulated by built in cable element. The mechanical parameters of surrounding rock and segmental lining are shown in Table 5. The mechanical parameters of interface element and cable element are shown in Table 6 and Table 7, respectively. Although the cable element can simulate the effect of improving the stress state of the surrounding rock after bolt is installed, it is difficult to simulate the effect of enhancing the mechanical properties of the surrounding rock (Bobet 2006; Liu et al. 2008; Wu et al. 2012). In order to reflect the reinforcing effects of grouted bolts, the mechanical parameters of bolted rock mass are determined according to the previous research results (Zhu et al. 1996), which are defined as Eq. (9).

$$\begin{cases} C_1 = C_0 + \eta \dfrac{\tau s}{ab} \\ \quad \varphi_1 = \varphi_0 \end{cases} \tag{9}$$

where C_1 and φ_1 are the cohesion and friction angle of bolted rock mass; C_0 and φ_0 are the cohesion and friction angle of original rock mass; η is empirical coefficient (2.0–5.0); τ is the shear strength of bolt; s is cross section area of bolt; a and b are annular and longitudinal spacing of bolts, respectively.

Table 5 Mechanics parameters for surrounding rock and segmental lining

Category	Modulus of deformation (MPa)	Poisson's ratio	Peak cohesion (MPa)	Peak friction angle (°)	Residual cohesion (MPa)	Residual friction angle (°)	Critical softening parameter
Similar material of limestone	250	0.27	0.11	54	0.01	30	0.012
Similar material of silty mudstone	68	0.3	0.042	36	0.004	20	0.025
Similar material of lining	330	0.25	–	–	–	–	–

Table 6 Mechanics parameters of interface element

Interface type	Normal stiffness (MPa/m)	Shear stiffness (MPa/m)	Cohesion (KPa)	Friction angle (°)	Tensile strength (KPa)
Limestone-lining	2e5	2e5	2	20	0
Silty mudstone-lining	1e5	1e5	2	20	0

Table 7 Mechanics parameters of cable element

Modulus of elasticity (MPa)	Poisson's ratio	Grout cohesion (KPa)	Grout friction angle (°)	Grout stiffness (MPa/m)
2e3	0.25	10	35	0.9

5.2 Calculation Results

The calculated displacement and stress have been transformed into the prototype displacement and stress according to the similarity principle.

5.2.1 Displacement Field

In order to analyze the influence of segmental lining-bolt combined support on the displacement under different surrounding rock conditions, the displacement distribution of surrounding rock in hard rock (monitoring section 1) and soft rock section (monitoring section 3) for the two test schemes are shown in Figs. 14 and 15, respectively. Compared with the vertical surrounding rock, the horizontal surrounding rock around the tunnel is more affected by excavation disturbance, especially in hard rock. Moreover, due to the low strength of soft rock, the excavation disturbance zone is more extensive than that of hard rock. When the segmental lining-bolt combined support is adopted in test scheme 2, the deformation of surrounding rock and the excavation disturbance zone are reduced obviously, no matter in hard rock or soft rock. In general, the displacement of the surrounding rock within 1.0D (D is the tunnel diameter) is significantly affected by excavation, which is consistent with the analysis of the test result.

5.2.2 Stress Field

The radial stress and tangential stress of each element are calculated by the stress transformation formula, the stress distribution of the surrounding rocks in hard rock (monitoring section 1) and soft rock (monitoring section 3) for the two test schemes is shown in Figs. 16 and 17, respectively.

From Figs. 16 and 17, it can be seen that

(1) After the excavation, the radial stress of the rock is released. The closer the distance from surrounding rock to the tunnel wall is, and the
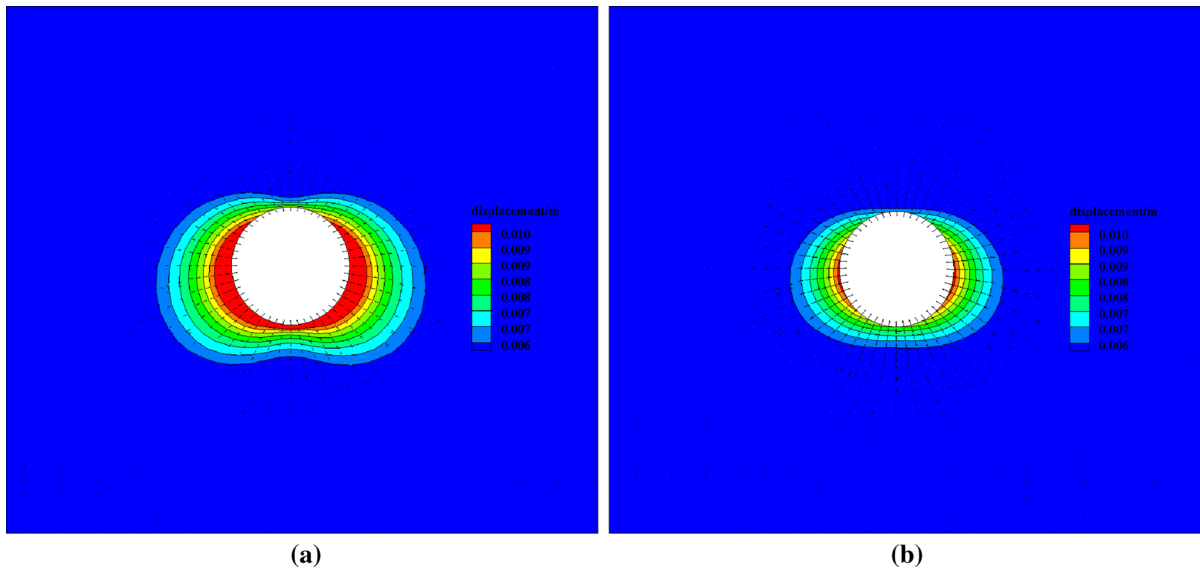
Fig. 14 Displacement contour of surrounding rock in hard rock. **a** Test scheme 1; **b** Test scheme 2
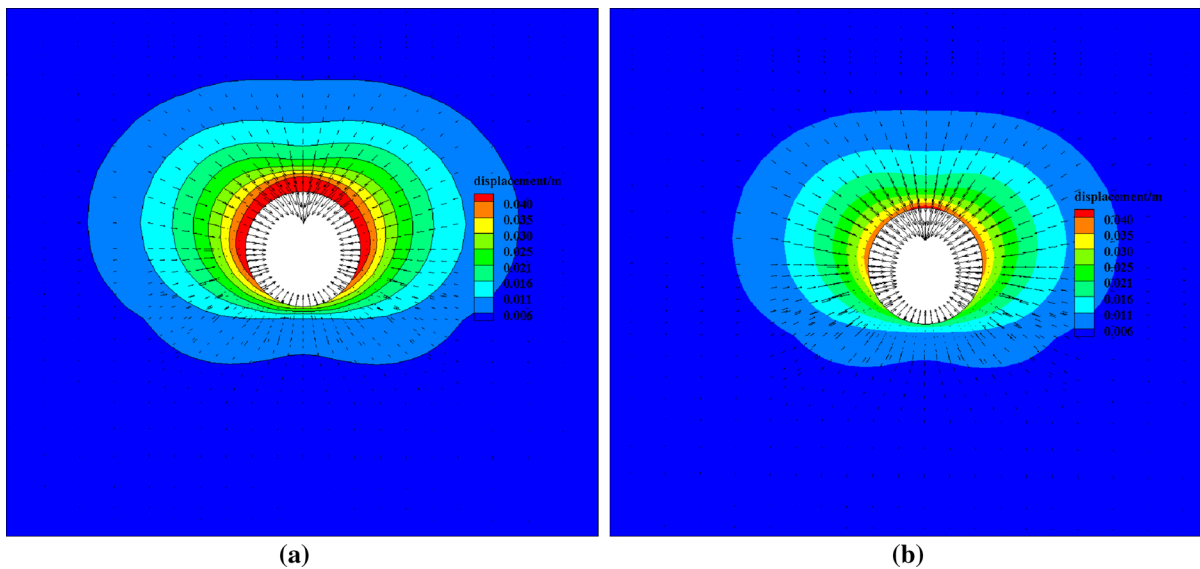

Fig. 15 Displacement contour of surrounding rock in soft rock. **a** Test scheme 1; **b** Test scheme 2

smaller the radial stress of surrounding rock is. The radial stress around the tunnel is presented as concentric circles of different diameters. The tangential stress of surrounding rock around the tunnel is concentrated and its distribution shape is complex. The tangential stress distribution of surrounding rock under different geological conditions is different. Compared with the horizontal direction, the stress of vertical

surrounding rock is more significant by the excavation disturbance, which is contrary to the influence of excavation disturbance on the deformation of surrounding rock.

(2) For hard rock, the tangential stress of surrounding rock around the tunnel decreases gradually along the tunnel radial direction except the vault and invert. When the segmental lining-bolt combined support is adopted, the tangential
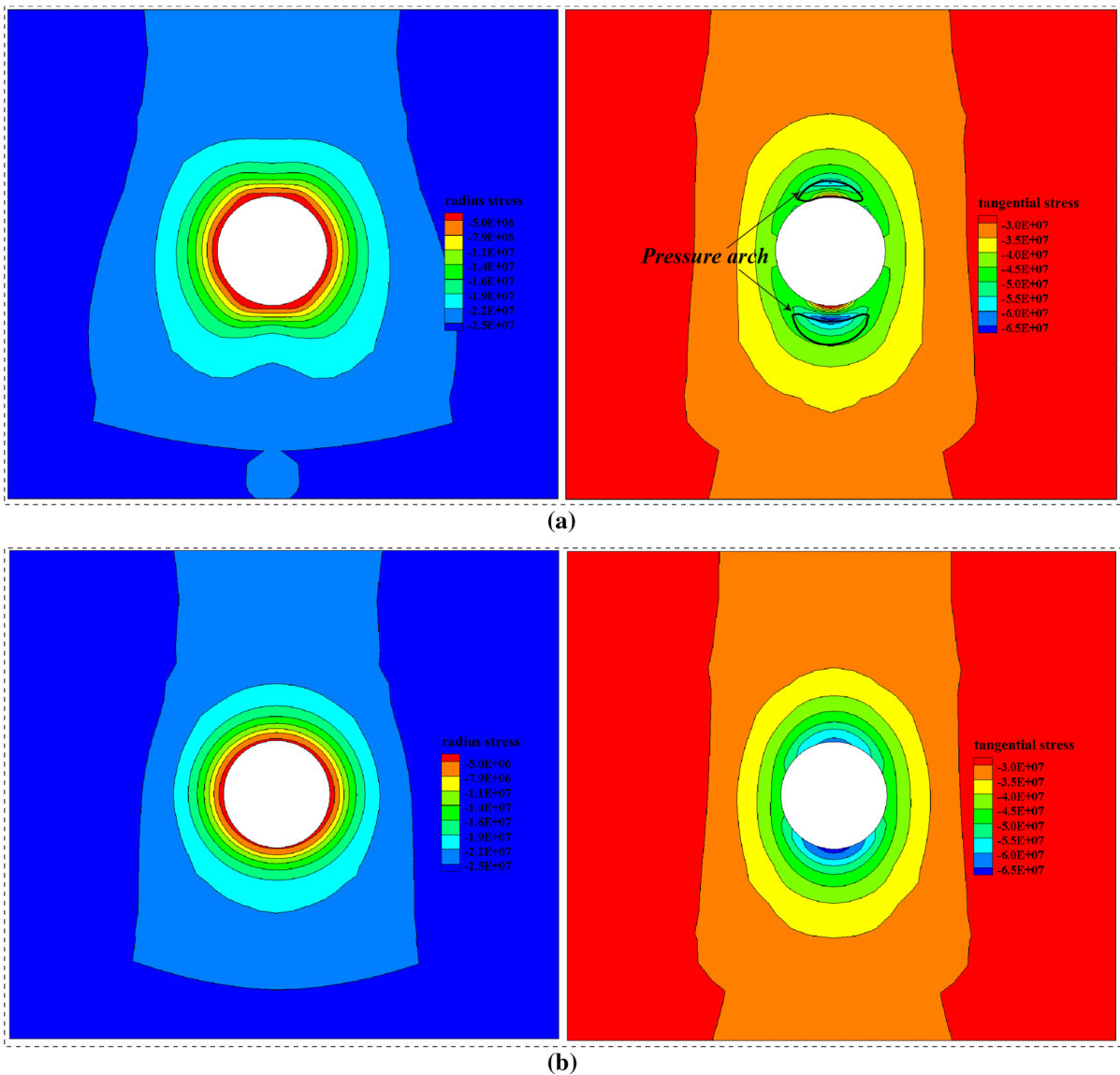
Fig. 16 Stress contour of the surrounding rock in hard rock. **a** Test scheme 1; **b** Test scheme 2

stress of surrounding rock around the tunnel decreases gradually along the tunnel radial direction. Because of the low strength of soft rock, plastic deformation occurs in soft rock for the two schemes. So the tangential stress of the surrounding rock increases at first and then decreases. The pressure arch of the surrounding rock penetrates each other in the deep surrounding rock to form an annular tangential stress concentration area. The reason is that the tangential stress of surrounding rock exceeds

the peak strength and enters the plastic softening stage after the tunnel excavation, which causes the stress of surrounding rock to move to the deep rock mass, thus forming a certain range of pressure arch. The released surrounding rock stress is mainly taken by the pressure arch. Generally, the lower the strength of the surrounding rock is, the farther the pressure arch formed around the tunnel from the tunnel wall is, the larger the area of pressure arch is, and the
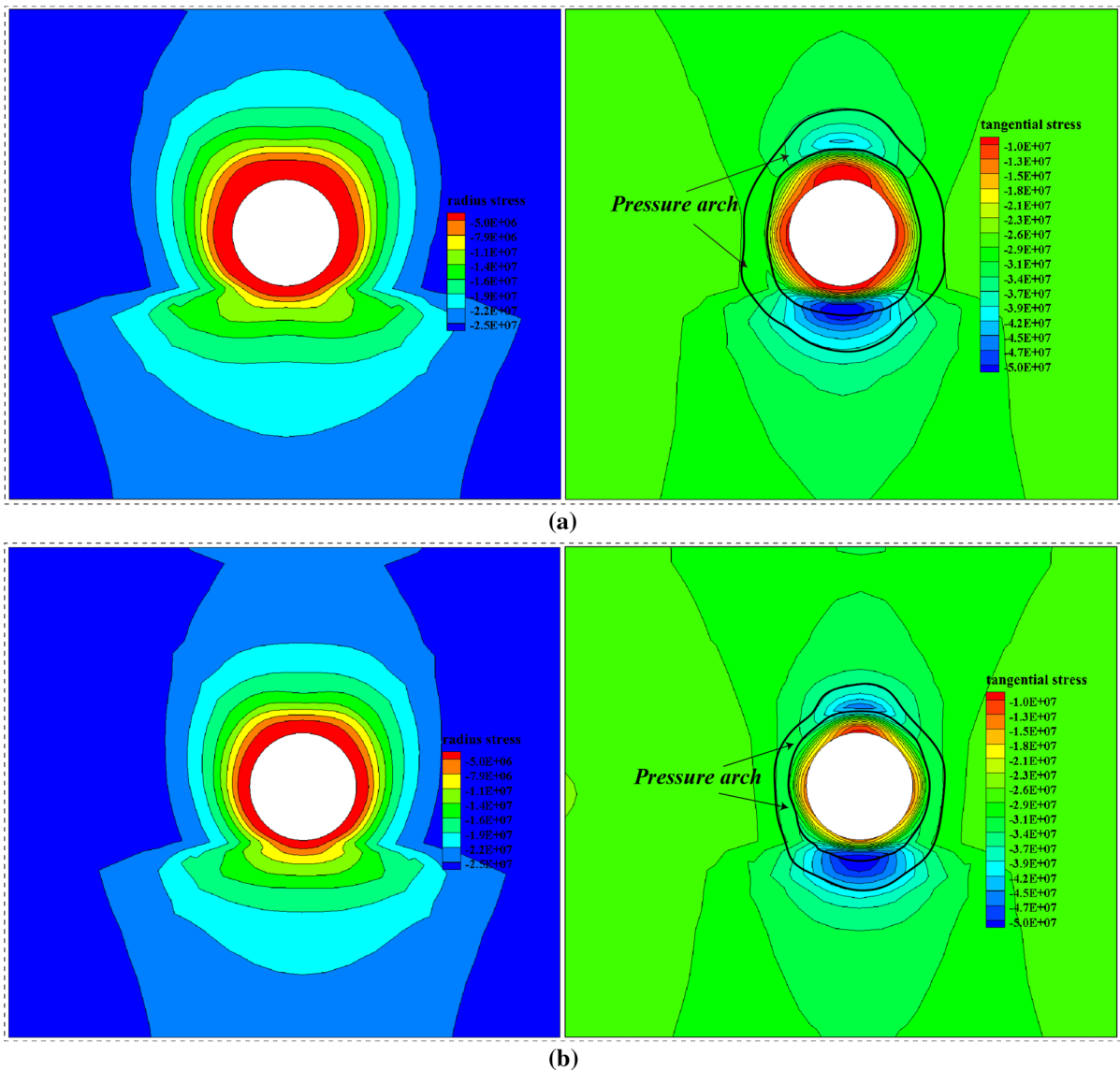
Fig. 17 Stress contour of the surrounding rock in soft rock. **a** Test scheme 1; **b** Test scheme 2

wider the disturbed zone of the surrounding rock is.

(3) Compared with test scheme 1, there is no pressure arch formed in hard rock when the segmental lining-bolt combined support is adopted in test scheme 2. However, with segmental lining-bolt combined support in soft rock, plastic deformation occurs in all parts around the tunnel, but the distance from pressure arch to tunnel wall and the area of pressure arch are obviously reduced. So the bolt

obviously improves the mechanical properties of surrounding rock and greatly improves the strength of surrounding rock.

5.2.3 Plastic Zone

The plastic zone distribution of the surrounding rock in hard rock (monitoring section 1) and soft rock (monitoring section 3) for the two test schemes is shown in Figs. 18 and 19, respectively.
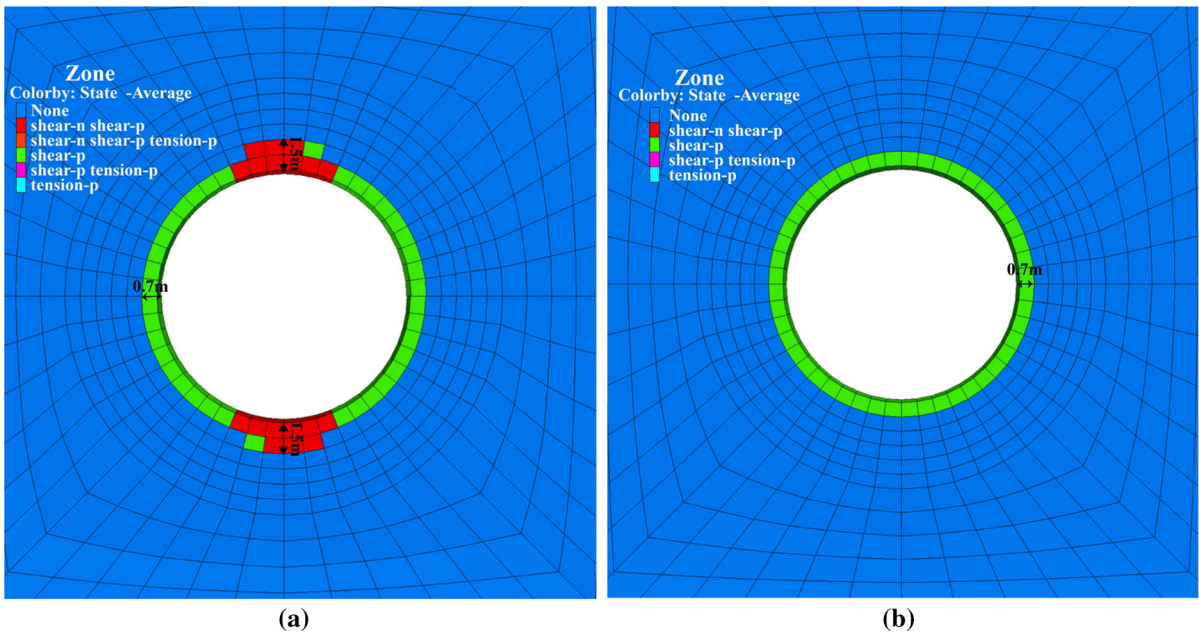
From Figs. 18 and 19, it can be seen that

Fig. 18 Plastic zone distribution of the surrounding rock in hard rock. **a** Test scheme 1; **b** Test scheme 2
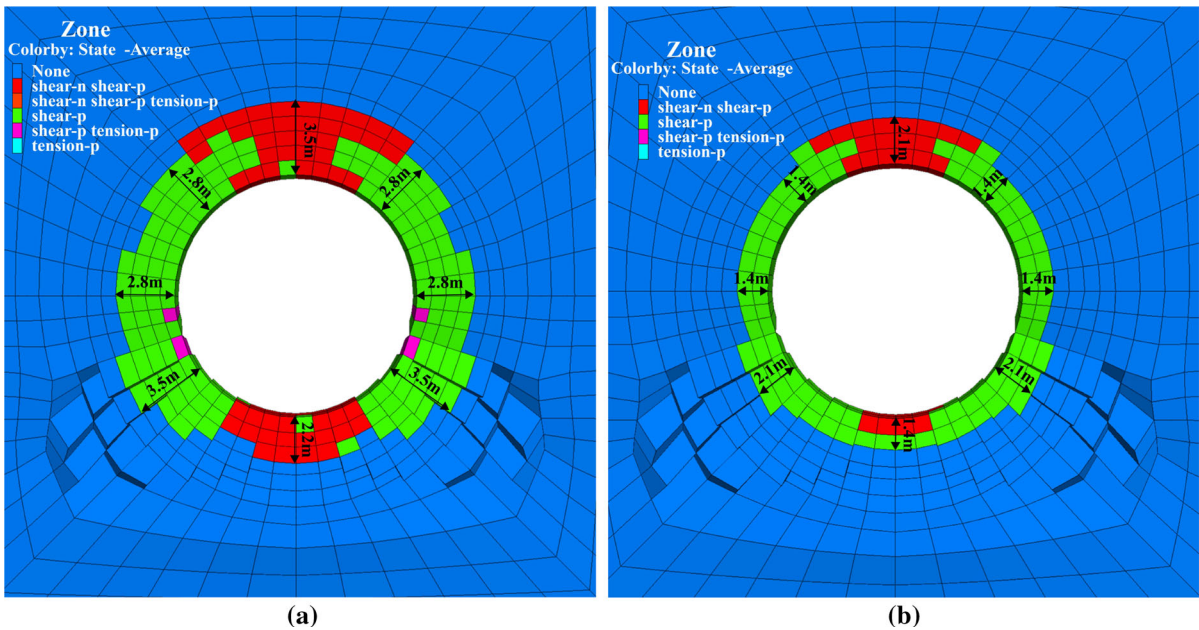

Fig. 19 Plastic zone distribution of the surrounding rock in soft rock. **a** Test scheme 1; **b** Test scheme 2

(1) For test scheme 1, besides forming a layer of plastic zone about 0.7 m thick around the tunnel in hard rock, a plastic zone about 1.5 m thick appears at the vault and invert. The area of plastic zone at the monitoring section 1 is about 26.3 m². However, the area of plastic zone of the surrounding rock on the monitoring

section 1 is about 22.56 m^2, which is reduced by about 14% for test scheme 2.

(2) For test scheme 1, the plastic zone of the surrounding rock around the tunnel in soft rock is larger than that in hard rock, and the depth of the plastic zone at the vault, the left spandrel and right spandrel is the largest, about 3.5 m. The plastic zone area of the surrounding rock at the monitoring section 3 is about 92 m^2. When the segmental lining-bolt combined support is adopted in test scheme 2, the depth of the plastic zone of surrounding rock at the monitoring section 3 is obviously reduced, and the area of plastic zone is about 52 m^2, which is reduced by about 43%. Compared with the hard rock, the support effect of the segment lining-bolt combined support is more significant for the surrounding rock in soft rock.

(3) Combined with the stress distribution of surrounding rock at the monitoring section 1 and section 3, it can be seen that there is a certain correlation between plastic zone and pressure arch. The depth and area of the plastic zone around the tunnel are obviously reduced after adopting the segmental lining-bolt combined support, and the pressure arch extent and the distance from the pressure arch to the tunnel wall are also reduced correspondingly at the corresponding position of the deep surrounding rock. It indicates that the plastic zone makes the stress of the surrounding rock move to the deep surrounding rock, thus inducing formation of the pressure arch. That is, the plastic zone is a necessary condition for the formation of pressure arch.

6 Mechanism of Segmental Lining-Bolt Combined Support

For any support structure, the object on which it works is always the surrounding rock. The surrounding rock itself is also a special support structure, so the surrounding rock and support are like a pair of contradictory bodies that seem to be opposite and unified. When studying the support mechanism of the support structure to the surrounding rock, it is necessary to consider the surrounding rock-support interaction. As two different types of support structure, the surrounding rock-segmental lining interaction and the surrounding rock-bolt interaction are essentially different. So the corresponding support mechanisms are also different. Taking into account results obtained by the model test and numerical calculation, the principle of the segmental lining-bolt combined support is shown in Fig. 20, where Fig. 20a is the support principle for bolt, Fig. 20b is the support principle for segmental lining, and Fig. 20c is the principle for segmental lining-bolt combined support.

As shown in Fig. 20a, the surrounding rock and bolt shrink into the tunnel together under the excavation load. The difference in stiffness between the surrounding rock and bolt makes the deformation of the surrounding rock much larger than that of the bolt. Due to the bonding effect of grout, the surrounding rock makes grout produce interface shear stress pointing to the tunnel, and the grout also causes the bolt to produce interface shear stress pointing to the tunnel, which is the above mentioned drawing shear stress. Under the action of drawing shear stress, the bonding shear stress opposite to the drawing shear stress is produced on the interface of the bolt in the deep surrounding rock, which makes the surrounding rock stress move to the deep rock. The drawing shear stress limits the deformation of the surrounding rock, which can be equivalent to providing the restraining reaction stress σ_m and applying the confining pressure to the surrounding rock. So the ultimate Mohr's stress circle of the surrounding rock is translated to the right along horizontal axis, which is stay away from the strength envelope. The bonding shear stress connects the shallow rock mass and the deep rock mass in series as a composite ring, and prevents the occurrence of shear rupture of the surrounding rock. Thus surrounding rock strength envelope is upwardly translated and slightly rotated counterclockwise, which means the cohesion and friction angle of the surrounding rock will increase. The bolt not only shares a part of the surrounding rock load to improve the surrounding rock stress state, but also strengthens the surrounding rock. The bolted rock mass forms a composite rock mass with higher strength and uniformity.

As shown in Fig. 20b, the all segments form a closed rigid load-bearing ring after the segmental linings are assembled. The surrounding rock converges into the tunnel and interacts with the segmental lining. With the continuous increase of surrounding
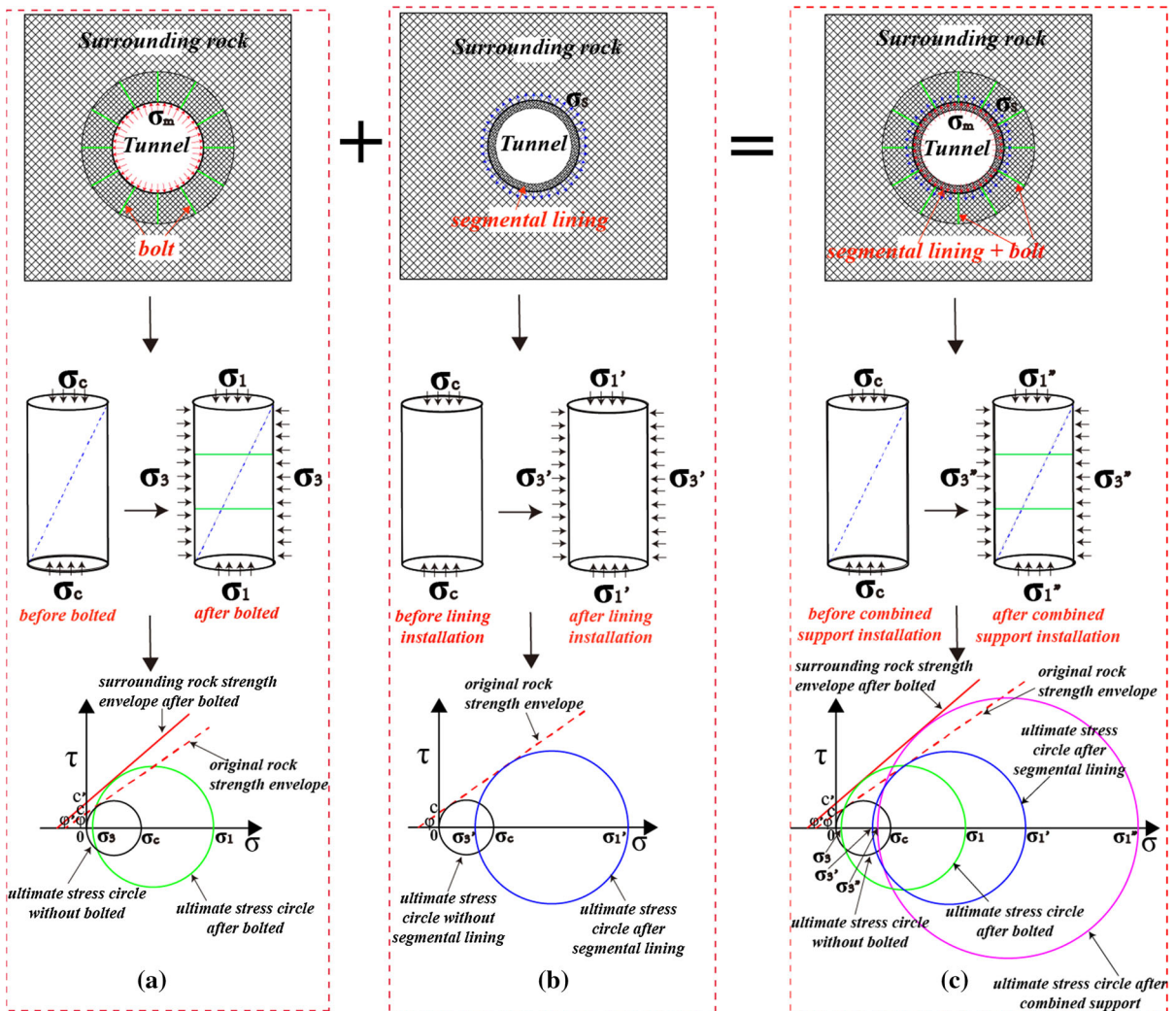
Fig. 20 Schematic diagram of principle of segmental lining-bolt combined support. **a** Principle of bolt support; **b** Principle of segmental lining; **c** Principle of segmental lining-bolt combined support

rock deformation, a part of excavation load moves to the deep surrounding rock to form pressure-bearing arch. The remaining excavation load transfers to the lining segment, which causes the stress and deformation of segmental lining. Because the stiffness of the lining segment is very large, the small deformation will provide a greater support resistance σ_s to the surrounding rock, which makes the surrounding rock come into the three-dimensional stress state from the two-dimensional stress state. The role of support resistance σ_s is equivalent that the segmental lining imposes a certain confining pressure on the tunnel wall, which make Mohr's stress circle of the surrounding rock translate to the right along horizontal

axis, thus far from the strength envelope of surrounding rock. So the segmental lining can not only take the excavation load with the surrounding rock, but also seal the surrounding rock to improve the stress state of surrounding rock, increase the bearing capacity of surrounding rock and limit the deformation development of surrounding rock.

Combined with the above analysis on the segmental lining and bolt, the principle of segmental lining-bolt combined support is shown in Fig. 20c. Segmental lining-bolt combined support contains the advantages of segmental lining and bolt. On the whole, the mechanism of segmental lining-bolt combined support mainly includes two aspects: (1) "load bearing

effect". During the surrounding rock and support system interaction, the segmental lining also provides the support resistance to surrounding rock, while the segmental lining takes the excavation load. Simultaneously, the bolt also provides the restraint reaction to surrounding rock by the drawing shear stress on the interface. The result of "support" is that the stress state of surrounding rock will be improved; (2) "protection and reinforcement effect". Bonding shear stress distributed on the rock-bolt interface integrates the shallow rock mass and deep rock mass in series, which restricts the development of surrounding rock shear fracture. The result of "protection and reinforcement" is that the mechanical properties and the bearing capacity of surrounding rock will be improved, and the proportion of load taken by support will be reduced. It also protects the support structure itself while protecting the surrounding rock.

7 Conclusion

(1) Based on the background of the Xianglushan Tunnel in Yunnan Water Diversion Project, the true three-dimensional geo-mechanical model test and numerical simulation for the construction of a deep tunnel through a weak fault are carried out. The stress and deformation of the surrounding rock and segmental lining, the distribution law of bolt axial force and rock-bolt interface stress are analyzed. The mechanism of segmental lining-bolt combined support is also proposed, which provides guidance for the establishment of construction scheme and the optimization of support design.

(2) The stress release of surrounding rock includes two forms: stress moving and stress transfer. The stress moving is that the excavation load released moves to the deep rock mass and forms a pressure arch, which is taken by the surrounding rock itself. The stress transfer is that the remaining excavation load is transferred to the support structure during the interaction of the surrounding rock and the support.

(3) There is a certain correlation between the plastic zone and the pressure arch. The plastic zone causes the surrounding rock stress to move to the deep surrounding rock, which induces the

formation of pressure arch. The larger the area of plastic zone is, the larger the extent of pressure arch formed in the deep surrounding rock is, and the farther the distance from pressure arch to the tunnel wall is. The plastic zone is the necessary condition for the formation of pressure arch in surrounding rock.

References

Arnau O, Molins C (2011) Experimental and analytical study of the structural response of segmental tunnel linings based on an in situ loading test. Part 2: numerical simulation. Tunn Undergr Space Technol 26:778–788

Barzegar M, Gharehdash S, Sharifzadeh M (2015) Numerical study of the behaviour of jointed tunnel lining. In: Proceedings of the 24th international mining congress of Turkey, TMMOB Maden Muhendisleri Odasi, pp 886–893

Bobet A (2006) A simple method for analysis of point anchored rockbolts in circular tunnels in elastic ground. Rock Mech Rock Eng 39:315

Cao YB (2014) Deformation-failure mechanism and bolt-shotcrete support of surrounding rock in large underground water sealed liquefied petroleum gas storage caverns. Dissertation, China University of Geosciences, Wuhan

Cheng LK (2014) Considerations and prospect of anchor-shotcrete support for underground water-sealed cavern. J Yangtze River Sci Res Inst 31:103–109

El Naggar H, Hinchberger SD, Lo K (2008) A closed-form solution for composite tunnel linings in a homogeneous infinite isotropic elastic medium. Can Geotech J 45:266–287

Funatsu T, Hoshino T, Sawae H, Shimizu N (2008) Numerical analysis to better understand the mechanism of the effects of ground supports and reinforcements on the stability of tunnels using the distinct element method. Tunn Undergr Space Technol 23:561–573

Gao Q, Song JG, Yu WJ, Wang ZH (2007) Design and numerical simulation of rock bolting and shotcrete for deep tunnels with high stress in Jinchuan mine. Chin J Geotech Eng 2:279–284

He MC, Xie HP, Peng SP, Jiang YD (2009) Study on rock mechanics in deep mining engineering. In: The 4th deep rock mechanics and engineering disaster control symposium and China university of mining and technology centennial academic conference. Beijing

Holmgren J, Ansell A (2006) Design of bolt anchored reinforced shotcrete linings subjected to impact loadings. In: The 10th international conference on shotcrete for underground support. British Columbia

Hu XY, He C, Wu D, Yang QJ (2018) Combined support technology of segment linings with compressible crushed stone and anchor bolts in layed rock. Chin J Geotech Eng 40:1093–1102

Huang W, Ma QY, Yuan WH, Yuan P (2011) Study on mechanism of bolt-shotcrete support and analysis of is mechanical properties in deep rock road way. Chin J Undergr Space Eng 7:28–32

Lee KM, Ge XW (2001) The equivalence of a jointed shield-driven tunnel lining to a continuous ring structure. Can Geotech J 38:461–483

Li SC, Liu Q, Li LP, Zhao Y, Wang HP, Zhao Y, Yan XS (2011) Development of large-scale geomechanical model test system for tunnel construction and its application. Chin J Rock Mech Eng 30:1368–1374

Liu HY, Small JC, Carter JP (2008) Full 3D modelling for effects of tunnelling on existing support systems in the Sydney region. Tunn Undergr Space Technol 23:399–420

Molins C, Arnau O (2011) Experimental and analytical study of the structural response of segmental tunnel linings based on an in situ loading test. Tunn Undergr Space Technol 26:764–777

Oliveir D, Diederichs MS (2017) Tunnel support for stress induced failures in Hawkesbury sandstone. Tunn Undergr Space Technol 64:10–23

Salemi A, Esmaeili M, Sereshki F (2015) Normal and shear resistance of longitudinal contact surfaces of segmental tunnel linings. Int J Rock Mech Min Sci 77:328–338

Sun Y, Zhang DL (2016) Synergy principle of complex supporting structure system in tunnel. Eng Mech 33:52–62

Sun HC, Zhang A, Shi ZH (2004) Mechanism of grouted rock bolting and self-supporting arch of tunnels. Chin J Geotech Eng 4:490–494

Wang KZ, Liu YR, Wang YP, Lin F, Yu CY (2014) Study of deformation characteristics of compound support steel arch and surrounding rock stability in diversion tunnel. Chin J Rock Mech Eng 33:217–224

Wen JZ, Yang CL, Su HT, Ning DB (2015) Theoretical analysis and application of composite arch for bolt-shotcrete steel frame supported tunnel in weak and fractured rock mass. China Civ Eng J 48:115–122

Wu WP, Feng XT, Zhang CQ, Qiu SL, Li ZH (2012) Reinforcing mechanism and simulating method for reinforcing effects of systemically grouted bolts in deep-buried hard rock tunnels. Chin J Rock Mech Eng 31:2711–2721

Xie HP (2017) Research framework and anticipated results of deep rock mechanics and mining theory. Adv Eng Sci 49:1–16

Yang Y (2015) Research on Mechanical characteristics of segment and bolt-shotcrete lining structure in inclined-shaft constructed by TBM (shield). Dissertation, China University of Mining and Technology, Beijing

Zhang PS, Yin K (2009) An analysis method of the whole working course for the force transferring mechanism in fixed segment of tensile-type anchor bar. Chin J Undergr Space Eng 5:716–723

Zhang QY, Li SC, Guo XH, Li Y, Wang HP (2008) Research and development of new typed cementitious geotechnical similar material for iron crystal sand and its application. Rock Soil Mech 8:2126–2130

Zhang QY, Zhang Y, Duan K, Liu CC, Miao YS, Wu D (2018) Large-scale geo-mechanical model tests for the stability assessment of deep underground complex under true-tri-axial stress. Tunn Undergr Space Technol 83:577–591

Zhu WS, Zhang YJ, Ren WZ (1996) Similar model block tests for reinforcing effeets of systematic bolts on rock mass of high slope of three gorges flight lock. Rock Soil Mech 2:1–6